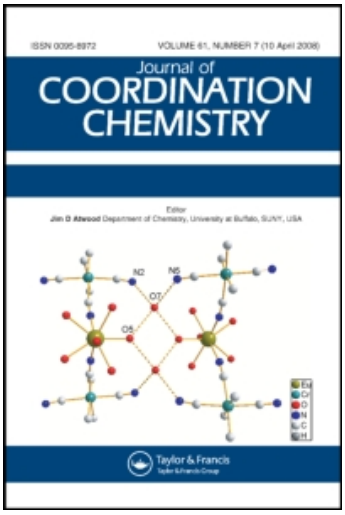

Journal of Coordination Chemistry
Publication details, including instructions for authors and subscription information:
http://www.informaworld.com/smpp/title~content=t713455674

Reactions of py[13]aneN$_4$ with the copper(II) complexes of diglycine and triglycine

Mansour M. Hassan[a]; Hayat M. Marafie[b]; Mohamed S. El-Ezaby[c]
[a] Chemistry Department, University of Aden, Aden-Crater PO Box 4848, Yemen [b] Chemistry Department, Kuwait University, 13060 Kuwait [c] Gulf University for Science and Technology, 13157 Kuwait

To cite this Article Hassan, Mansour M. , Marafie, Hayat M. and El-Ezaby, Mohamed S.(2004) 'Reactions of py[13]aneN$_4$ with the copper(II) complexes of diglycine and triglycine', Journal of Coordination Chemistry, 57: 7, 553 — 569
To link to this Article: DOI: 10.1080/00958970410001696834
URL: http://dx.doi.org/10.1080/00958970410001696834

J. Coord. Chem., Vol. 57, No. 7, 10 May 2004, pp. 553–569

REACTIONS OF PY[13]ANEN$_4$ WITH THE COPPER(II) COMPLEXES OF DIGLYCINE AND TRIGLYCINE

MANSOUR M. HASSAN[a,*], HAYAT M. MARAFIE[b,*] and MOHAMED S. EL-EZABY[c]

[a]*Chemistry Department, University of Aden, Aden-Crater PO Box 4848, Yemen;*
[b]*Chemistry Department, Kuwait University, PO Box 5969 Safat, 13060 Kuwait;*
[c]*Gulf University for Science and Technology, PO Box 29623 Safat, 13157 Kuwait*

(Received 14 April 2003; Revised 15 September 2003; In final form 04 March 2004)

Ligand exchange reactions between the pyridine-containing macrocycle 3,7,10,16-tetraazabicyclo[10,3,1]-hexadeca-1,(16),12,14,-triene, py[13]aneN$_4$, and the Cu(II) complexes of diglycine (GG) and triglycine (GGG) have been investigated in aqueous solution. The kinetics were studied by stopped-flow techniques at 25°C and $I = 0.2\,\mathrm{M}\,(KNO_3)$. A single kinetic step was observed at the d–d transition band (λ_{max} = 580 nm) for the Cu(II) macrocycle. All kinetic measurements were carried out under pseudo first-order conditions in the pH range 5.0–6.2 with the ligand concentration at least 10-fold excess. The specific rate constant, k_i, for the two systems studied describes the reaction between the 1 : 1 Cu(II)-polyglycine complex and the monoprotonated form, LH^+, of the macrocycle. Cu(II)-GGG complexes exchange the metal more rapidly than the corresponding Cu(II)-GG complexes:

$$\mathrm{CuGG\ (or\ GGG)^+ + LH^+ \rightarrow Cu\,L + GG\ (or\ GGG)^-}; \qquad k_1$$
$$\mathrm{CuGG\ (or\ GGG)\,H_{-1} + LH^+ \rightarrow Cu\,L + GG\ (or\ GGG)^-}; \qquad k_2$$

where $k_1 = 9.1 \times 10^5$ and $5.8 \times 10^6\,\mathrm{M^{-1}\,s^{-1}}$ and $k_2 = 2.5 \times 10^5$ and $1.3 \times 10^6\,\mathrm{M^{-1}\,s^{-1}}$ for the GG and GGG systems, respectively. The reaction mechanisms of these reactions are discussed. Formation constants for the ternary systems Cu-GG-py[13]aneN$_4$ and Cu-GGG-py[13]aneN$_4$ are evaluated by pH-electrode titrations in aqueous solution at 25°C and $I = 0.2\,\mathrm{M}\,(KNO_3)$. Attempts to separate the solid ternary compounds from the blue perchlorate solution mixture of Cu(II), py[13]aneN$_4$ and GG (or GGG) were unsuccessful. Instead, red plate-shaped crystals separated from the blue solution. The crystal structure of the red compound [Cu(py[13]aneN$_4$)](ClO$_4$)$_2$ was determined.

Keywords: Diglycine; Triglycine; Copper(II); Macrocycle

INTRODUCTION

Ligand–ligand replacement reactions of the general type

$$\mathrm{ML_a + L_b \rightarrow ML_b + L_a}$$

*Corresponding authors. E-mails: abdulhameedmansour@hotmail.com; marohayat@hotmail.com

ISSN 0095-8972 print: ISSN 1029-0389 online © 2004 Taylor & Francis Ltd
DOI: 10.1080/00958970410001696834

(where M is a metal ion and L_a and L_b are different ligands) are of considerable interest from a mechanistic point of view because of their importance in biological applications [1,2]. Earlier studies have revealed that these reactions generally proceed through the formation of intermediates in which the incoming ligand is partially coordinated and the leaving group is partially dissociated. As a result of detailed analysis of such mechanisms, it is now possible to predict the rate of ligand–ligand exchange reactions. There is an inverse relationship between the thermodynamic stability of the reactant complex and its reactivity, found to be applicable for open-chain ligands [3] as well as for cyclic polyamines [4].

In an attempt to check the validity of this rule for a large number of chelators with different donor atoms, a study was carried out on the kinetics of the reaction of cyclam (1,4,8,11-tetraazacyclotetradecane) with a series of Cu(II) complexes for which the formation constants (K_{CuL}) span over 15 orders of magnitude [5]. The study concluded that for complexes with formation constants greater than 10^{10}, there is an inverse relationship between K_{CuL} and their reactivities towards cyclam. However, for less thermodynamically stable complexes, reactivity and stability are independent of each other.

The apoproteins or apoenzymes of a large number of metalloproteins or metalloenzymes are normally prepared by extracting the metals with a chelating agent such as 1,10-phenanthroline. In a recent study [6], the kinetics of the of 14-, 15- and 16-membered tetraaza macrocycles with Cu(II)-diglycine were determined. It was concluded that metalloproteins with stability constants greater than 10^{10} react relatively slowly with the monoprotonated form LH^+ of these macrocycles.

The macrocyclic ligand py[13]aneN_4 forms stable complexes with biologically important metal ions such as Cu(II) and Zn(II). The formation constants ($\log K_{ML}$) for the Cu(II) and Zn(II) complexes of this macrocycle are 20.14 and 14.27, respectively [7]. The present study examines equilibria and ligand exchange kinetics of the reaction of py[13]aneN_4 with the Cu(II) complexes of the diglycine (GG) and the triglycine (GGG).

EXPERIMENTAL

Syntheses

The ligand 3,7,10,16-tetraazabicyclo[10,3,1]-hexadeca-1,(16),12,14,-triene, py[13]aneN_4, was synthesized in the hydrobromide form (py[13]ane$N_4 \cdot 3HBr$) according to a literature method [8]. Anal. calcd for $C_{12}H_{23}N_4Br_3$: C, 31.13%; H, 5.01%; N, 12.10%. Found: C, 30.91%; H, 4.99%; N, 12.20%.

The complex of py[13]aneN_4 with Cu(II) was prepared as follows: to a mixture of py[13]aneN_4 (0.463 g, 1.0 mmol) and GGG (0.757 g, 4.0 mmol) in H_2O (50 mL), $Cu(NO_3)_2 \cdot 2\frac{1}{2}H_2O$ (0.233 g, 1.0 mmol) was added while stirring. The pH was then adjusted to about 11 by adding dilute NaOH solution. After 1 h of stirring at room temperature, $NaClO_4 \cdot H_2O$ (1.4 g, 10.0 mmol) was added and the mixture was stirred for another 0.5 h. A small amount of EtOH was added to the final mixture and the mixture was then transferred to a large evaporating dish and allowed to evaporate slowly at room temperature. After 24 h of slow crystallization, red plate-shaped crystals separated. Anal. calcd for $C_{12}H_{20}Cl_2CuN_4O_8$: C, 29.8%; H, 4.1%; N, 11.6%.

TABLE I Crystal data and data collection, structure solution and refinement parameters for $Cu[C_{12}N_4H_{20}](ClO_4)_2$

Chemical formula	$C_{12}H_{20}Cl_2CuN_4O_8$
Formula weight	482.76
Crystal system	Triclinic
Space group	$P\bar{1}$
Unit cell dimensions	$a = 8.1024(7)$ Å; $\alpha = 90.389(2)^\circ$ $b = 8.6569(8)$ Å; $\beta = 105.846(2)^\circ$ $c = 14.0182(12)$ Å; $\gamma = 111.960(2)^\circ$
Volume	870.71(13) Å^3
Z, Z'	2, 1
Density (calculated)	1.841 mg m^{-3}
Wavelength	0.71073 Å
Temperature	100(2) K
$F(000)$	494
Absorption coefficient	1.614 mm^{-1}
Absorption correction	Semiempirical from equivalents
Max. and min. transmission	0.9684 and 0.7179
Theta range for data collection	2.56 to 30.53°
Reflections collected	6536
Independent reflections	4706 [R(int) = 0.0252]
Data / restraints / parameters	4706/220/327
wR (F^2 all data)	$wR_2 = 0.1675$
R (F obsd data)	$R_1 = 0.0684$
Goodness-of-fit on F^2	1.026
Observed data [$I > 2\sigma(I)$]	3486
Largest and mean shift/s.u.	0.000 and 0.000
Largest diff. peak and hole	2.678 and −1.420 e Å^{-3}

$wR_2 = \{\Sigma[w(F_o^2 - F_o^2)^2]/\Sigma[w(F_o^2)^2]\}^{1/2}$.
$R_1 = \Sigma| |F_o| - |F_c| | / \Sigma|F_o|$.

Found: C, 29.6%; H, 3.9%; N, 11.4%. The structure of the solid was determined by X-ray analysis. The data are presented in Table I.

Materials and Procedures

Cu(II) nitrate solution was standardized against EDTA (AR, Aldrich) using a copper electrode and calomel reference electrode. The stock solution of the ligand py[13]aneN_4 was standardized potentiometrically against the standard Cu(II) nitrate solution using a copper/calomel electrode system. The titration was carried out in ammonia buffer at pH 10. The Cu(II) di- and triglycinate solutions were prepared from Cu(II) nitrate and the corresponding peptides (1 : 2 mole ratio) in 0.05 M MES (2-[*N*-morpholino]ethanesulphonic acid; SIGMA buffer) for use in the kinetic studies. KOH and HCl solutions were used to adjust the pH in the range 5.00–6.25. A colour change from blue to violet took place on amide deprotonation (pH > 6). The solutions were freshly prepared for each set of kinetic measurements. The ionic strength was maintained at 0.2 M KNO_3.

Kinetic Measurements

The kinetics for reaction of the Cu(II) di- and triglycine complexes with the macrocycle ligand py[13]aneN_4 were measured spectrophotometrically at the maximum absorption wavelength of 580 nm, using a Hi-Tech MG-6000 Rapid Diode Array Stopped Flow Spectrophotometer (SF-41) interfaced with an IBM PC. Data acquisition and

processing were carried out using Hi-Tech systems kinetics software. Rate constants were calculated by the computer programs IS-software from Hi-Tech. The initial concentration of the Cu(II) polyglycinate was 1×10^{-3} M and that of the macrocycle, L_T, was varied between 0.01 and 0.06 M. The observed rate constants were the average of at least five kinetic runs taken at a given pH and L_T.

Potentiometric Measurements

Potentiometric titrations were performed under N_2 gas at 25°C on a Brinkmann Metrohm 736 GB Titrino equipped with an ORION Ross combination electrode (model 81-02). The electrode was standardized by three buffer calibrations using Titrino's internal standardization method. The potentiometric measurements, in the pH range *ca.* 2–11, were made on 50.0 mL of the macrocycle ligand [$(0.50–1.0) \times 10^{-3}$ M]. The ionic strength was maintained at 0.2 M (KNO_3). The pH data were obtained (triply collected) after additions of 0.01 mL increments of standard KOH solution (with a 20–60 s equilibration time) while the titration data (pH *vs.* mL base) were captured using the Titrino's built-in software. Direct pH meter readings were used for calculation of the mixed protonation constants (also known as Brønsted constants), which involve the hydrogen ion activity and the concentration of the other species. Solutions of the binary (1 : 1) and the ternary (1 : 4 : 1) systems Cu(II)-py[13]aneN_4, Cu(II)-GG(or GGG) and Cu(II)-GG(or GGG)-py[13]aneN_4 were similarly titrated against standard KOH solution. The titration data were collected and treated with the SUPERQUAD program [9] for the determination of the protonation and formation constants. Species distribution diagrams were generated using the program HYSS [10].

Spectral Measurements

The spectral changes associated with isomerization of the red complex [red-Cu(py[13]aneN_4)]$^{2+}$ into the blue complex [blue-Cu(py[13]aneN_4)]$^{2+}$ in aqueous solution were monitored in the UV–visible region by using a conventional spectrophotometer (Cary-3 Bio UV–Vis spectrophotometer interfaced with an IBM PC).

RESULTS AND DISCUSSION

The protonation equilibria of the macrocyclic ligand py[13]aneN_4 can be represented as follows:

$$\begin{aligned}
&L + H^+ \rightleftharpoons LH^+; && K_1 = [LH^+]/[L][H^+] \\
&LH^+ + H^+ \rightleftharpoons LH_2^{2+}; && K_2 = [LH_2^{2+}]/[LH^+][H^+] \\
&LH_2^{2+} + H^+ \rightleftharpoons LH_3^{3+}; && K_3 = [LH_3^{3+}]/[LH_2^{2+}][H^+] \\
&LH_3^{3+} + H^+ \rightleftharpoons LH_4^{4+}; && K_4 = [LH_4^{4+}]/[LH_3^{3+}][H^+]
\end{aligned}$$

where K_1, K_2, K_3 and K_4 are the practical stepwise constants.

The protonation constants are summarized in Table II. Protonation constant K_4 of the ligand could not be determined from the potentiometric measurements because of the low range of pH values (< 2) required for reliable calculation. Speciation curves for the ligand py[13]aneN_4 are shown in Fig. 1.

Calculation of the 1 : 1 complex of Cu(II) with the macrocyclic ligand revealed a log formation constant equal to 16.56 which is less by *ca.* 3.5 log units than the value reported previously [7]. The difference may be attributed to the difference in the experimental conditions and the methodology of obtaining the titration data. The reported value was obtained by competitive experimental methods using trien as the competitive ligand at $I = 0.1$ M (KNO_3) and 25°C.

In the titration curves of a 1 : 1 mole ratio of Cu(II) : GG (both are 1×10^{-3} M) with potassium hydroxide, the first equivalence point occurs above pH 6 after the addition of two equivalents of the base (Fig. 2a), which is attributed to the formation of $CuGGH_{-1}H_2O$ [11] with the dissociation of two protons from both the protonated amino group and the peptide nitrogen. A second, relatively flat buffer region is followed by a weak inflection after addition of a further equivalent of base, attributable to deprotonation of the coordinated water molecule, that is

$$CuGGH_{-1}H_2O \rightleftharpoons (CuGGH_{-1}OH)^{-1} + H^+; \quad K_{OH} \tag{1}$$

TABLE II Protonation and formation constants involved in the systems pCu(II)-qPy[13]aneN_4(L)-rGG or GGG-sH (where p, q, r and s are the stoichiometric coefficients) at 25°C and $I = 0.2$ M KNO_3

Species	*p*	*q*	*r*	*s*	*log β*		
					This work	*Literature values*	
GG-H	0	0	1	1		8.22	[12]
	0	0	1	2		11.46	[12]
GGG-H	0	0	1	1		8.06	[12]
	0	0	1	2		11.42	[12]
L-H	0	1	0	1	9.73 ± 0.01	9.79	[7]
	0	1	0	2	18.26 ± 0.03	18.28	[7]
	0	1	0	3	21.79 ± 0.08	21.13	[7]
	0	1	0	4	–	< 22.13	[7]
Cu(II)-L-H	1	1	0	0	16.56 ± 0.00	20.14	[7]
Cu(II)-GG-H	1	0	1	0		5.87	[12]
	1	0	1	−1		1.4	[12]
	1	0	1	−2		−7.87	[12]
	2	0	2	−1		11.86	[15]
Cu(II)-GGG-H	1	0	1	0		5.23	[12]
	1	0	1	−1		−0.26	[12]
	1	0	1	−2		−7.02	[12]
	1	0	1	−3		−18.06	[12]
Cu(II)-L-GG-H	1	1	1	2	30.50 ± 0.05		
	1	1	1	0	19.29 ± 0.01		
	1	1	1	−1	10.18 ± 0.06		
Cu(II)-L-GGG-H	1	1	1	2	31.51 ± 0.04		
	1	1	1	0	20.46 ± 0.02		
	1	1	1	−1	12.22 ± 0.07		

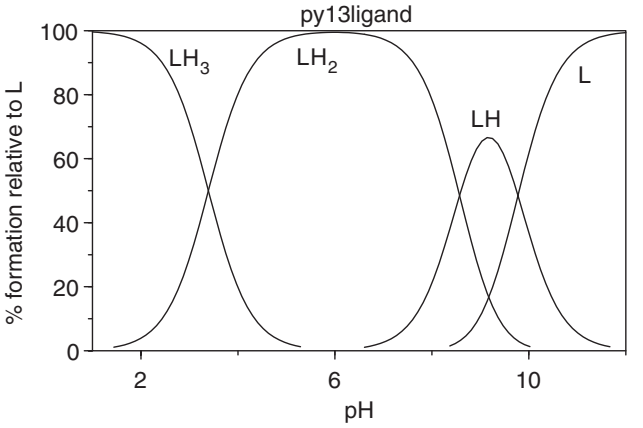

FIGURE 1 Speciation curves for protonation of py[13]aneN_4 at 25°C and $I = 0.2$ M KNO_3.

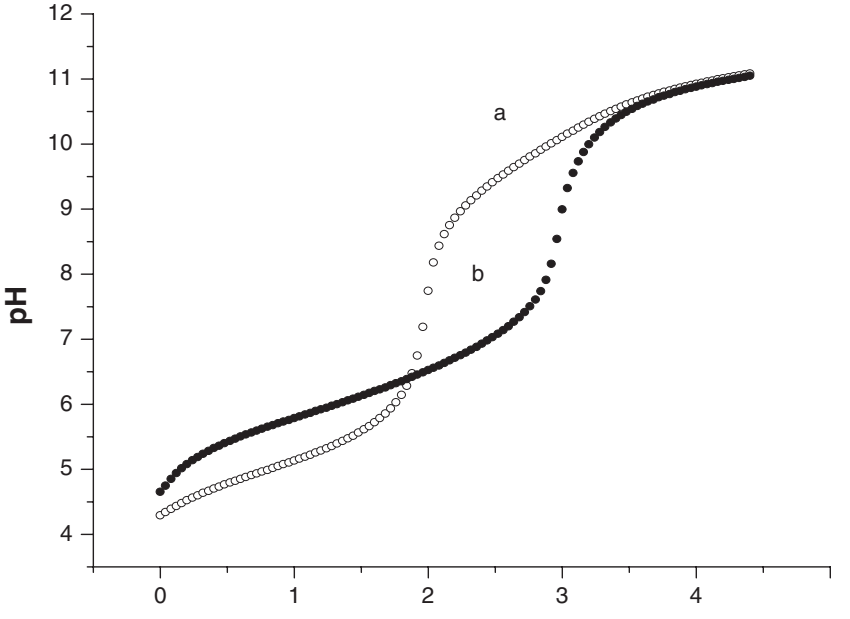

FIGURE 2 Potentiometric titration curves for Cu(II)-peptides (1 : 1 mixtures, 1.0×10^{-3} M) (a) Cu(II)GG and (b) Cu(II)GGG at 25°C and $I = 0.2$ M KNO_3, where B = mol KOH/mol macrocycle ligand.

In addition, dimerization may also occur in solution, i.e.

$$2\,\mathrm{CuGGH_{-1}H_2O} \rightleftarrows (\mathrm{GGH_{-1}Cu\text{-}OH\text{-}CuGGH_{-1}})^{-} + \mathrm{H^{+}} + \mathrm{H_2O}; \quad K_{\mathrm{D}} \qquad (2)$$

However, in the titration curve of Cu(II) triglycine (Fig. 2b), the equivalence point occurs after addition of three equivalents of base due to formation of $(\mathrm{CuGGGH_{-2}(H_2O)})^{-}$ with the dissociation of three protons, one from the protonated amino group and two from the two peptide linkages. Other equilibria may also exist in solutions of pH > 6 [12].

The speciation curves for the Cu(II)-diglycine and Cu(II)-triglycine complexes are shown in Figs. 3a and 3b, respectively.

Simulation of the potentiometric data from the ternary systems using SUPERQUAD indicated the presence of ternary species. The stoichiometries and the formation constants of these species are depicted in Table II. Speciation curves of the Cu(II)-GG(or GGG)-macrocycle (1 : 4 : 1) are shown in Figs. 4a and 4b.

Preparation and Structure Determination of [Cu(py[13]aneN$_4$)](ClO$_4$)$_2$

The mixing of Cu^{2+}, Cu(II)GG^+ or Cu(II)GGG^+ complexes with py[13]aneN$_4$ in aqueous percholorate solution usually resulted in formation of an intense blue solution. However, the solid that separated was always red in colour and was identified as [Cu(py[13]aneN$_4$)](ClO$_4$)$_2$. The complex crystallizes in the triclinic space group $P\bar{1}$

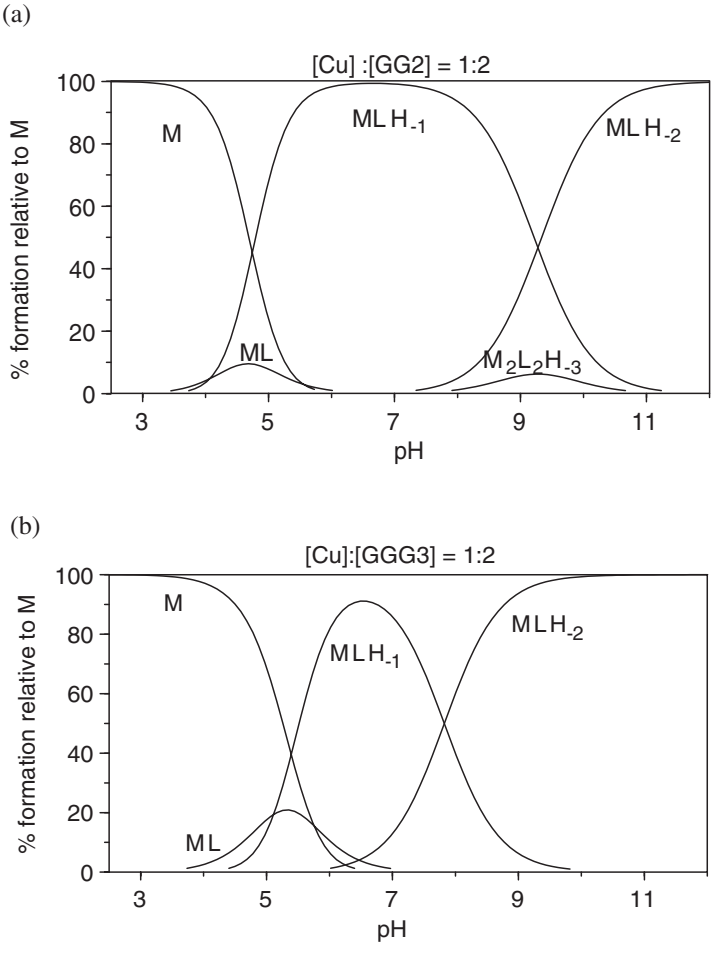

FIGURE 3 (a) Speciation curves for Cu(II) diglycine: [Cu] = 0.5[GG] = 0.001 M at 25°C and I = 0.2 M KNO_3. ML = $[CuGG]^+$, MLH_{-1} = $[CuGGH_{-1}]$, $M_2L_2H_{-3}$ = $[GGH_{-1}Cu\text{-}OH\text{-}CuGGH_{-1}]^-$, MLH_{-2} = $[CuGGH_{-1}(OH)]^-$. (b) Speciation curves for Cu(II) triglycine: [Cu] = 0.5[GGG] = 0.001 M at 25°C and I = 0.2 M KNO_3. ML = $[CuGGG]^+$, MLH_{-1} = $[CuGGGH_{-1}]$, MLH_{-2} = $[CuGGGH_{-2}]^-$.

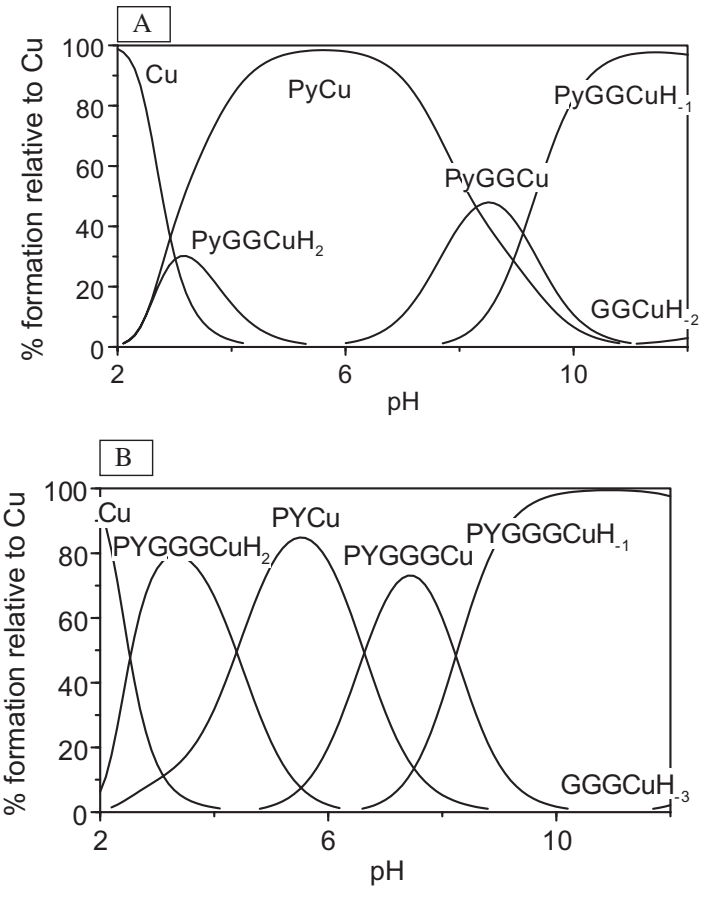

FIGURE 4 Concentration distribution of the complexes formed in the systems (a) Cu(II)-GG-py[13]aneN$_4$ ([Cu] = 1/4[GG] = [py[13]aneN$_4$] = 0.001 M) and (b) Cu(II)-GGG-py[13]aneN$_4$ ([Cu] = 1/4[GGG] = [py[13]aneN$_4$] = 0.001 M) as a function of pH.

with unit cell dimensions (angles): $a = 8.1024(7)$ Å ($\alpha = 90.389(2)^\circ$), $b = 8.6569(8)$ Å ($\beta = 105.846(2)^\circ$), $c = 14.0182(12)$ Å ($\gamma = 111.960(2)^\circ$). Figure 5 shows the structure of the red complex and Table III depicts the bond lengths and angles of Cu(II) with the ligating atoms. The structure of the complex shows that Cu(II) is tetracoordinated (CuN_4 chromophore), with the central metal ion and the pyridine N in a plane and the three Ns of the macrocycle zigzagging above and below this plane. The parent crystal structure of [Cu(py[13]aneN$_4$)](ClO$_4$)$_2$ shown in Fig. 5 indicates that the complex crystallizes as two isomers of almost equal ratio. Each of these two isomers has the five- and six-membered rings pointing in opposite directions in comparison with the other isomer (Fig. 6).

When the red solid was dissolved in water, a red solution was obtained ($\lambda_{max} = 510$ nm, $\varepsilon = 123.1\ M^{-1}\,cm^{-1}$); however, when left for an hour or heated, it turned to the original intense blue–violet colour ($\lambda_{max} = 580$ nm, $\varepsilon = 146.4\ M^{-1}\,cm^{-1}$). This was attributed to isomerization. The spectral changes associated with isomerization from the red to blue complex are shown in Fig. 7. The marked blue shift exhibited by the red complex indicates the tendency of Cu(II) to be in the plane with the macrocycle nitrogens (square

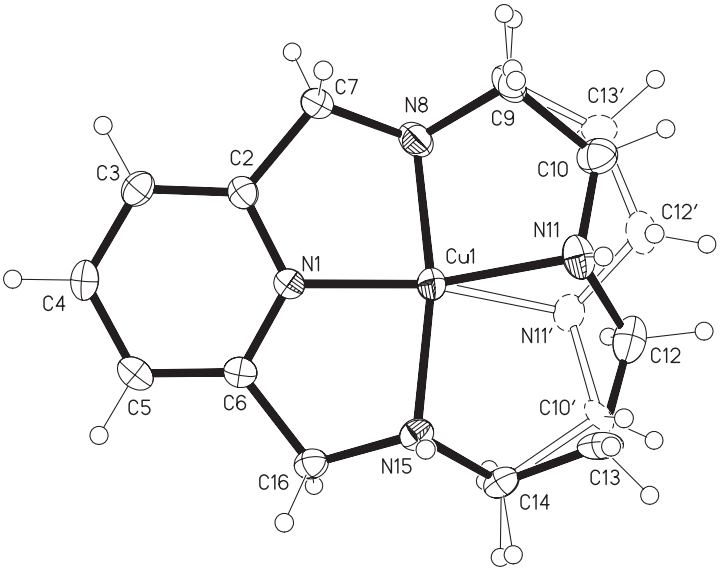

FIGURE 5 Crystal structure of $[Cu(py[13]aneN_4)(red)](ClO_4)_2$.

TABLE III Bond lengths (Å) of Cu(II) with the ligating atoms and angles (°) involved

Cu(1)–N(1)	1.876(4)
Cu(1)–N(8)	1.993(4)
Cu(1)–N(15)	2.002(4)
Cu(1)–N(11′)	1.970(8)
Cu(1)–N(11)	1.959(8)
N(1)–Cu(1)–N(11)	166.8(2)
N(1)–Cu(1)–N(11′)	163.5(2)
N(11)–Cu(1)–N(11′)	29.6(3)
N(1)–Cu(1)–N(8)	84.65(16)
N(11)–Cu(1)–N(8)	86.6(3)
N(11′)–Cu(1)–N(8)	103.5(2)
N(1)–Cu(1)–N(15)	83.71(15)
N(11)–Cu(1)–N(15)	105.0(3)
N(11′)–Cu(1)–N(15)	87.7(2)
N(8)–Cu(1)–N(15)	168.35(16)

planar). The blue complex could be a folded form with the pyridine nitrogen donor in an axial position or the complex distorted such that the copper atom lies out of the plane of the four nitrogen donors. The failure in separating the ternary complex species from the Cu(II)peptide-py[13]aneN$_4$ solutions, though detected in the equilibrium study (see above and Table II), could be attributed to the relative higher solubility of the ternary over the binary complex species.

Kinetics and Reaction Mechanism

A fast kinetic step was observed at 580 nm in acidic media. The step was in the time range 50–200 ms and was dependent on both pH and the initial concentration of the macrocycle, L_T. Subsequent slow steps were usually observed in basic solution, which

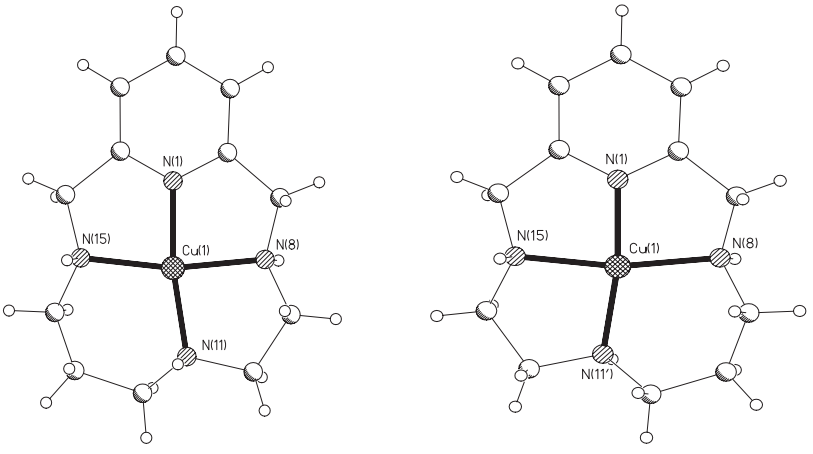

FIGURE 6 The two isomers of $[Cu(py[13]aneN_4)](ClO_4)_2$.

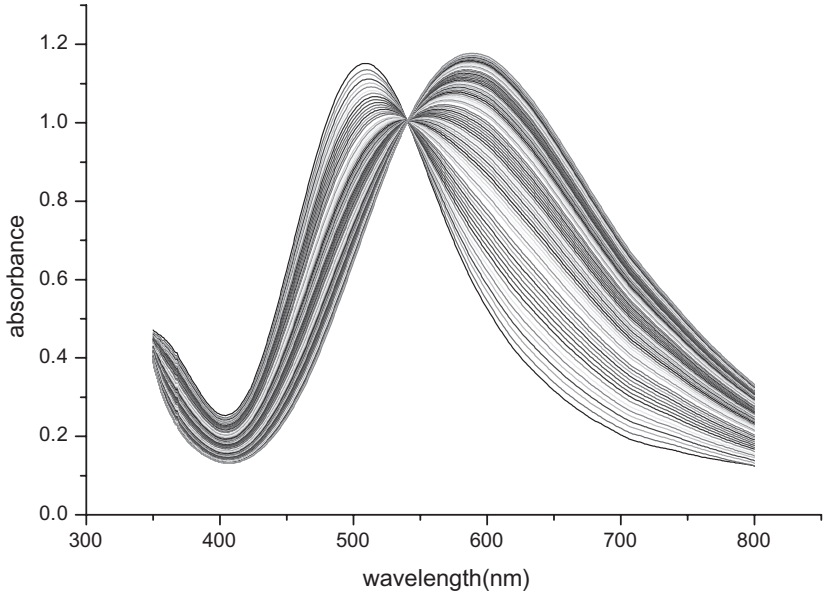

FIGURE 7 Time-resolved spectra of the conversion of $[Cu(py[13]aneN_4)(red)]^{2+}$ to $[Cu(py[13]aneN_4)(blue)]^{2+}$ in aqueous solution at 25°C, $t_{1/2} = 27.5$ min.

may be due to the inversions of chiral *sec*-NH centres in the macrocyclic complex to give the most thermodynamically stable configuration.

The monitored reaction is shown in Equation (3):

$$\text{Cu(II)peptides} + L_T \rightarrow CuL_T + \text{peptides}; \quad k_f \tag{3}$$

where Cu(II)peptides represent the total Cu(II) diglycine or total Cu(II) triglycine and L_T is the total macrocycle concentration. The kinetics could be fitted to the following rate expression

$$\text{Rate} = k_f(\text{Cu(II)peptides})(L_T)$$

where k_f is the experimental second-order rate constant for the exchange reaction. A series of kinetic runs were carried out at several pH values under conditions where $L_T \gg$ (Cu(II)peptides), that is:

$$[d(CuL_T)/dt]_{pH} = k_{obs}(Cu(II)peptides) \quad (4)$$

for which the observed first-order rate constants, k_{obs}, could be obtained from the integrated form

$$\ln(CuL_T)/[(CuL_T)_e - (CuL_T)_t] = \ln A_e/(A_e - A_t) = k_{obs}t \quad (5)$$

where $(CuL_T)_t$ and $(CuL_T)_e$ represent the total concentration of the Cu(II) macrocyclic complex at time t and at equilibrium, respectively, A_t and A_e are the corresponding values of the absorbance of $(CuL_T)_t$ and $(CuL_T)_e$ measured at the d–d transition band ($\lambda_{max} = 580$ nm) and t is the elapsed time for each measurement of A_t.

Values of k_{obs} for the two Cu(II)peptides reaction with the macrocycle ligand are summarized in Table IV. The pH dependence of k_{obs} for the complexation of py[13]aneN$_4$ with Cu(II)peptides is shown in Fig. 8a,b.

Plots of k_{obs} *vs.* L_T at various pH values are linear (Fig. 9a,b), with slopes equal to k_f at various pH values and intercepts of negligible magnitudes ($\sim$ zero) so that,

$$k_{obs} = k_f(L_T) \quad \text{(at a given pH)}$$

TABLE IV Values of k_{obs} for the reaction of py[13]aneN$_4$ with Cu(II)GG or Cu(II)GGG complexes at 25°C and $I = 0.2$ M KNO$_3$

pH	*[py[13]aneN$_4$] (M)*	*k_{obs} (s^{-1})*	*pH*	*[py[13]aneN$_4$] (M)*	*k_{obs} (s^{-1})*
Cu(II)GG					
5.00	0.010	1.82	5.00	0.019	3.61
5.50	0.010	2.41	5.50	0.019	4.22
5.75	0.010	4.05	5.75	0.019	7.55
5.90	0.010	5.32	5.90	0.019	10.6
6.00	0.010	8.40	6.00	0.019	15.6
6.15	0.010	11.4	6.15	0.019	22.2
6.25	0.010	19.1	6.25	0.019	36.2
5.00	0.016	2.80	5.00	0.025	4.45
5.50	0.016	3.45	5.50	0.025	5.43
5.75	0.016	5.61	5.75	0.025	9.22
5.90	0.016	8.62	5.90	0.025	13.4
6.00	0.016	12.8	6.00	0.025	20.1
6.15	0.016	17.8	6.15	0.025	28.6
6.25	0.016	29.4	6.25	0.025	46.3
Cu(II)GGG					
5.60	0.010	25.1	5.60	0.019	49.5
5.85	0.010	35.3	5.85	0.019	69.8
5.95	0.010	45.3	5.95	0.019	87.5
6.10	0.010	64.2	6.10	0.019	118
6.20	0.010	76.4	6.20	0.019	145
5.60	0.016	40.1	5.60	0.025	66.9
5.85	0.016	57.6	5.85	0.025	91.8
5.95	0.016	73.2	5.95	0.025	116
6.10	0.016	97.5	6.10	0.025	152
6.20	0.016	120	6.20	0.025	188

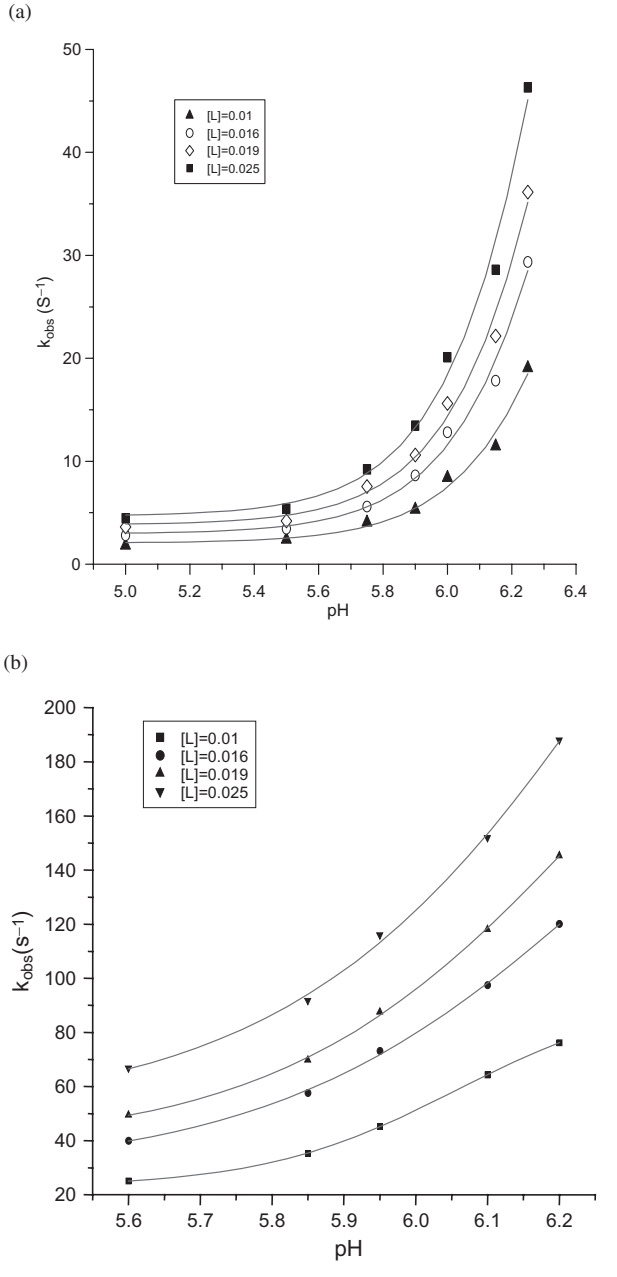

FIGURE 8 pH dependence of k_{obs} for the complexation of py[13]aneN_4 with (a) Cu(II) diglycine and (b) Cu(II) triglycine at 25°C and $I = 0.2$ M KNO_3.

Cu(II)-diglycine complex $(CuGG)^+$

Previous studies [5,13,14] have shown that the monoprotonated forms of tetraazamacrocycles, LH^+, are several orders more reactive than the higher protonated species, even for reactions in which the concentration of the LH^+ species is less than

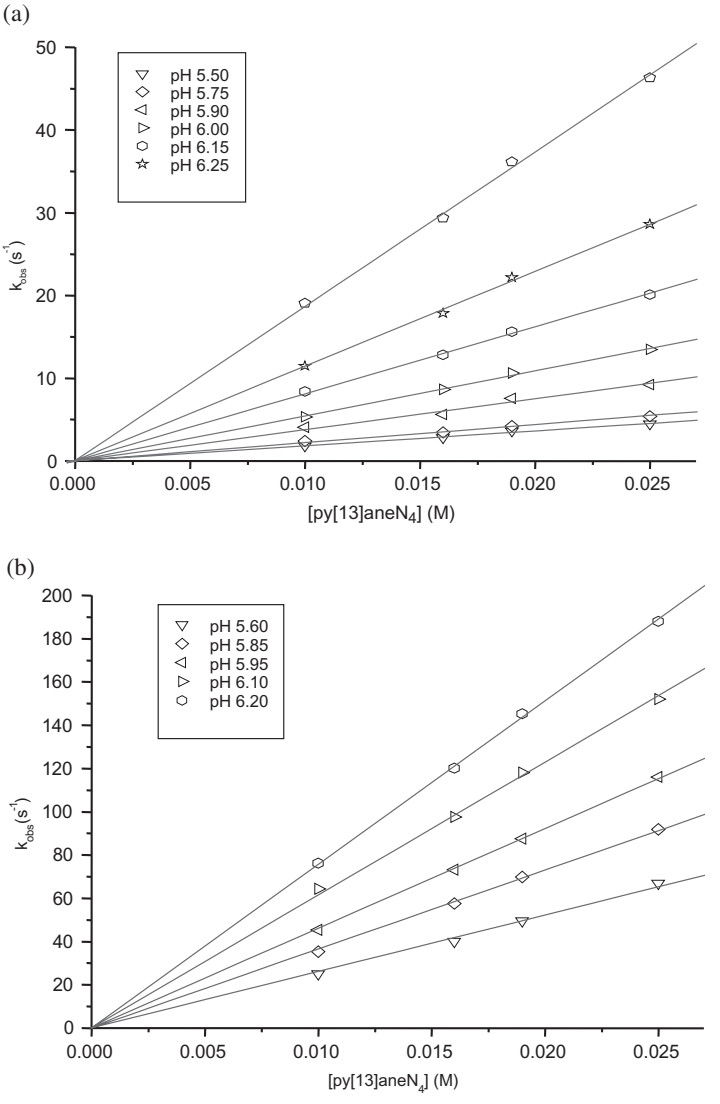

FIGURE 9 Plots of k_{obs} *vs* the total concentration of py[13]aneN$_4$ for reaction with (a) Cu(II)-diglycine complexes and (b) Cu(II)-triglycine complexes at 25°C and $I = 0.2$ M KNO_3, at different pH values.

0.01% of LH_2^{+2} [13]. If it is assumed that the reactions of the species LH_3^{+3}, LH_2^{+2} and L with Cu(II) diglycine (CuGG) are not kinetically significant in the pH range used in this work, the kinetically important reactions are those shown in Scheme 1.

In the pH range 5.00–6.25

$$L_T = (LH_2^{2+}) = (LH^+)(H^+)K_2 \tag{6}$$

The total concentration of Cu(II)GG is given by

$$(CuGG)_T = (CuGG)^+ + (CuGGH_{-1}) \tag{7}$$

By appropriate substitution in Equations (6) and (7) it can be readily shown that

$$k_f K_2[(H^+) + K_{-H1}] = k_1 + k_2 K_{-H1}/(H^+) \quad (8)$$

The equilibrium constant K_{-H1} (due to amide deprotonation of the diglycine) has a value of 8.51×10^{-5} at 25°C and $I = 0.2$ M. The constant K_2 (the second protonation constant of the ligand) is equal to 3.39×10^8 (Table II). Values of the various parameters in Equation (8) are given in Table V. A straight line with negative intercept and slope equal to 25.8 ± 1.3 was obtained when $k_f K_2[(H^+) + K_{-H1}]$ was plotted against $(H^+)^{-1}$ (Fig. 10a). This implies that k_1 has approximately zero value and k_2 a value of $(3.0 \pm 1.8) \times 10^5\ M^{-1} s^{-1}$ at 25°C and $I = 0.2$ M. The results indicate that the Cu(II)-diglycine species [$CuGGH_{-1}$] is the reactive species in the formation of the Cu(II)-macrocycle complex (reaction B, Scheme 1).

Cu(II)-triglycine complex $(CuGGG)^+$

Analogous measurements were carried out on Cu(II) triglycine, Cu(II)GGG, giving the data shown in Table IV. Following the same strategy used above for Cu(II)GG and by assuming that LH_2^{2+} is the only significant species in the pH range of measurements, the kinetically important reactions are shown in Scheme 2.

Equation (6) also applies here and the total concentration of Cu(II)GGG is given by

$$(CuGGG)_T = (CuGGG)^+ + (CuGGGH_1) + (CuGGGH_{-2})^- \quad (9)$$

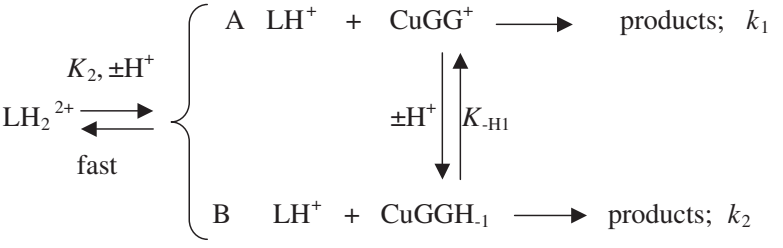

SCHEME 1

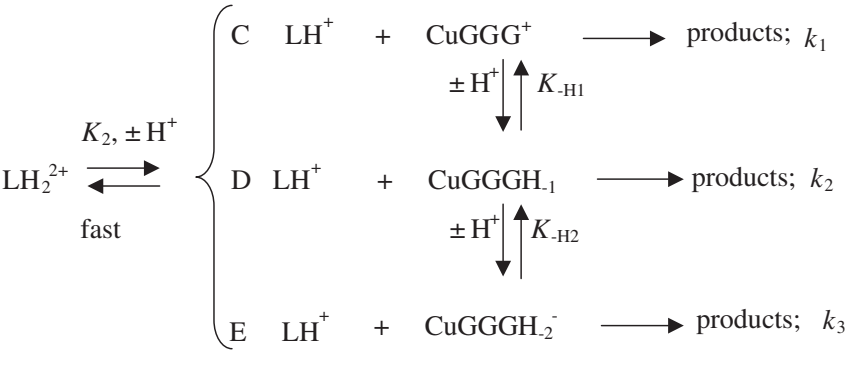

SCHEME 2

TABLE V Values of the various parameters in Equation (8)

pH	$10^5(a_H=[H^+])$	$10^5([H^+]+K_{-H1})$	k_f	$10^{-10}(k_fK_2)$	$10^{-6}(k_fK_2([H^+]+K_{-H1}))$
5.50	0.316	8.83	203	6.88	6.08
5.75	0.178	8.69	356	12.1	10.5
5.90	0.126	8.64	546	18.5	16.0
6.00	0.100	8.61	785	26.6	22.9
6.15	0.071	8.58	1156	39.2	33.6

By appropriate substitution in Equations (6) and (9) it can be readily shown that

$$k_f K_2[(H^+) + K_{-H1} + K_{-H1}K_{-H2}] = k_1 + k_2K_{-H1}/(H^+) + k_3K_{-H1}K_{-H2}/(H^+)^2 \quad (10)$$

A plot of the right-hand side of Equation (10) *vs.* $(H^+)^{-1}$ should be quadratic, with the first, second and third coefficients corresponding to k_1, k_2K_{-H1} and $k_3K_{-H1}K_{-H2}$, respectively. However, the regression analysis of Equation (10) instead yielded a straight line (Fig. 10b), with an intercept equal to $(5.8 \pm 0.8) \times 10^6\,M^{-1}\,s^{-1}$ $(=k_1)$ and slope equal to 11.0 ± 0.5 $(=k_2K_{-H1})$, which gives $k_2 = (1.3 \pm 0.5) \times 10^6\,M^{-1}\,s^{-1}$. This finding indicates that reaction E in Scheme II is insignificant in the formation of the Cu(II) macrocycle complex. This may be attributed to the lower concentration of the species $CuGGGH_{-2}$ in the pH range of study (less than 2% at pH 6.2) (Fig. 3b).

The rate constants k_1 and k_2 for the Cu(II)-diglycine and the Cu(II)-triglycine systems are summarized in Table VI along with the literature values for the reaction of the LH^+ of cyclam with $CuGGH_{-1}$ and a number of other Cu(II)-aminocarboxylate complexes.

CONCLUSIONS

Table VI summarizes the rate constants found in this work together with pertinent constants from other systems. The following general conclusions can be extracted from the table.

(i) Reactions of protonated species of py[13]aneN_4 with the Cu(II)-peptide complexes show no changes in reactivity towards the positively charged complexes, $CuGG^+$ and $CuGGG^+$, and the neutral complexes, $CuGGH_{-1}$ and $CuGGGH_{-1}$. This indicates that the reactions of protonated py[13]aneN_4 with the Cu(II)-peptide complexes have negligible electrostatic effects. The same observation was reported previously [5] for the reactions of LH^+ of cyclam with the complexes of Cu^{2+}_{aq}, CuG^+ and CuIDA (G = glycinate; IDA = iminodiacetate).

(ii) The relatively high reactivity of $CuGGG^+$ over $CuGGGH_{-1}$ may be interpreted in terms of the number of coordinating groups; the peptide acts as bidentate ligand in the first complex and tridentate in the latter.

(iii) The charge and the number of coordinating groups effects mentioned in (i) and (ii) operate simultaneously and counteract each other.

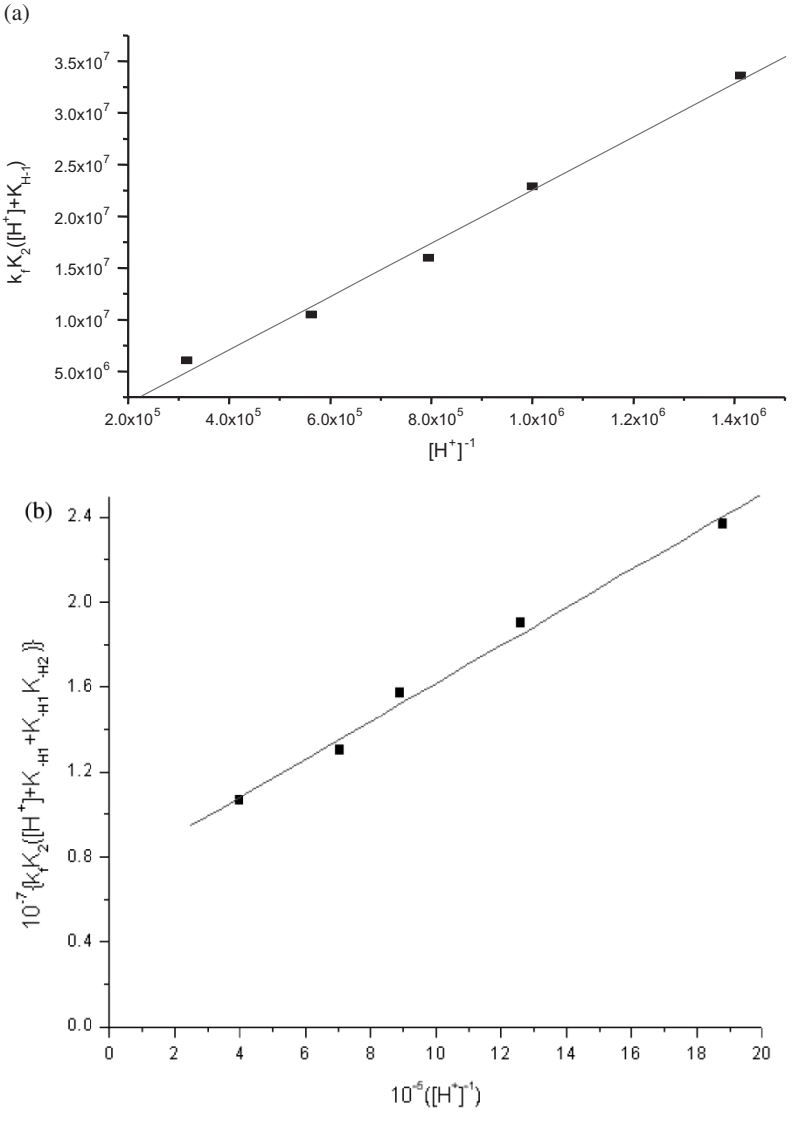

FIGURE 10 (a) Plot of $k_f K_2[(H^+) + K_{-H1}]$ *vs* $(H^+)^{-1}$. (b) Plot of $k_f K_2[(H^+) + K_{-H1} + K_{-H1}K_{-H2}]$ *vs* $(H^+)^{-1}$ (Equations (8) and (10)).

(iv) The $CuGGGH_{-1}$ complex exchanges copper more readily than $CuGGH_{-1}$. This may be correlated with the relative stabilities of these complexes; $CuGGGH_{-1}$ is less stable than $CuGGH_{-1}$ (Table II).

(v) The LH^+ species of py[13]aneN_4 reacts with $CuGGH_{-1}$ 100 times faster than the LH^+ species of cyclam with the same complex. This rate difference can be rationalized in terms of both the relative stability of the first protonation constant [$\log K^1_H$(cyclam) = 11.45 [14] and $\log K^1_H$(py[13]aneN_4) = 9.73] and ligand topology. Thus, perhaps the added rigidity of py[13]aneN_4, due to incorporation of the pyridine moiety, provides the favoured framework for Cu(II) over that of cyclam.

TABLE VI Rate constants for the reaction of monoprotonated species (LH^+) of py[13]aneN$_4$ and cyclam with Cu-peptides and Cu-aminocarboxylate complexes

Complex	$k_1\,(M\,s)^{-1}$	$k_2\,(M\,s)^{-1}$	$\log K_{ML}$; $\log K_{ML-H1}$
py[13]*aneN*$_4$			
$[Cu(H_2O)_6]^{2+}$ [a]	$(2.5 \pm 0.1) \times 10^7$		
[Cu-diglycinate]$^{(+/0)}$	$(9.1 \pm 0.9) \times 10^5$	$(2.5 \pm 2.8) \times 10^5$	5.50; 1.43
[Cu-triglycinate]$^{(+/0)}$	$(5.8 \pm 0.8) \times 10^6$	$(1.3 \pm 0.5) \times 10^6$	5.08; −0.03
Cyclam			
[Cu-diglycinate]^0 [b]	–	3.0×10^3	
$[Cu(H_2O)_6]^{2+}$ [c]	2.4×10^6		
$[CuG]^+$ [c]	2.0×10^6		
[CuIDA] [c]	3.7×10^6		
$[CuNTA]^-$ [c]	8.4×10^4		

[a] Unpublished results; [b] Ref. 6; [c] Ref. 3.
IDA, iminodiacetate; NTA, nitrilotriacetate.

(vi) Displacement of peptides from the Cu(II)-peptides studied in this work probably involves initial coordination of the macrocycle at the site occupied by the aquo ligand followed by rapid displacement of the adjacent carbonyl or carboxylate donor.

Acknowledgment

We thank Dr D.H. Busch of the Department of Chemistry at the University of Kansas for providing research facilities for this work and for fruitful discussions.

References

[1] A.D.J. Sherry, *J. Less-Common Metals* **149**, 133 (1989).
[2] A.D.J. Sherry and C.F.G.C. Geralds, In: J.C.G. Bunzeli and G.R. Choppin (Eds), Lanthanides Probes in Life, Chemical and Earth Sciences, Theory and Practice (Elsevier, Amsterdam, 1989), Chapter 4.
[3] R.M. Shepherd, G.M. Hodgson and D.W. Margerum, *Inorg. Chem.* **10**, 989 (1971).
[4] M. Kodama and E. Kimura, *J. Chem. Soc., Dalton Trans.* 247 (1978).
[5] Y. Wu and T.A. Kaden, *Helv. Chim. Acta* **68**, 1611 (1985).
[6] R.W. Hay and M.M. Hassan, *J. Coord. Chem.* **37**, 271 (1996).
[7] J. Costa and R. Delgado, *Inorg. Chem.* **32**, 5257 (1993).
[8] H. Stetter, W. Frank and R. Mertens, *Tetrahedron* **37**, 767 (1981).
[9] P. Gans, A. Sabatini and A. Vaca, *J Chem. Soc., Dalton Trans.* 1195 (1985).
[10] L. Alderighi, P. Gans, A. Ienco, D. Peters, A. Sabatani and A. Vacca, *Coord. Chem. Rev.* **184**, 311 (1999).
[11] M. Sato, S. Matsuki, M. Ikeda and J.-I. Nakaya, *Inorg. Chim. Acta* **125**, 49 (1986).
[12] A.E. Martell and R.M. Smith, Critical Stability Constants (New York, Plenum Press, 1974), Vol. 1, pp. 294 and 322.
[13] S.P. Kasprzyk and R.G. Wilkins, *Inorg. Chem.* **21**, 3349 (1982).
[14] A.P. Leugger, L. Hertli and T.A. Kaden, *Helv. Chim. Acta* **61**, 2296 (1978).
[15] H.M. Marafie, M.S. El-Ezaby, M. Rashad and N.M. Moussa, *Polyhedron* **3**, 787 (1984).